Supporting Information

Unprecedented three-dimensional 10-connected bct nets based on trinuclear secondary building units and their magnetic behavior

Zhi Su, You Song, Zheng-Shuai Bai, Jian Fan, Guang-Xiang Liu, Wei-Yin Sun*

Coordination Chemistry Institute, State Key Laboratory of Coordination Chemistry, School of Chemistry and Chemical Engineering, Nanjing National Laboratory of Microstructures, Nanjing University, Nanjing 210093, China,

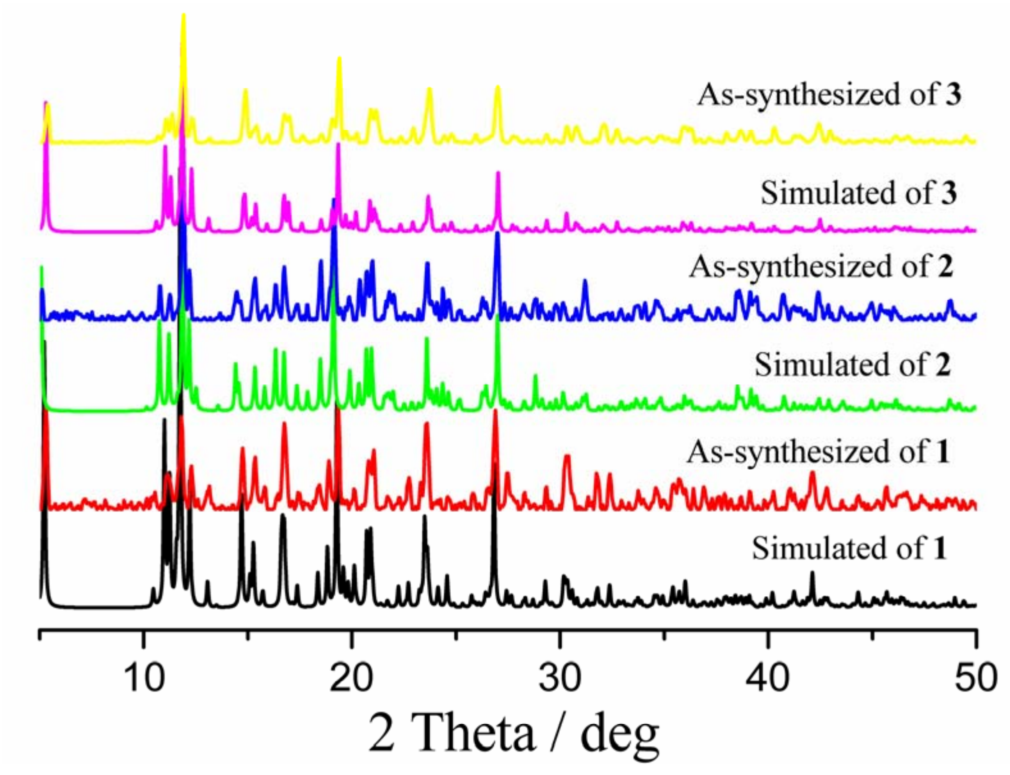

Figure S1. The simulated and as-synthesized XRPD patterns of **1** - **3**.

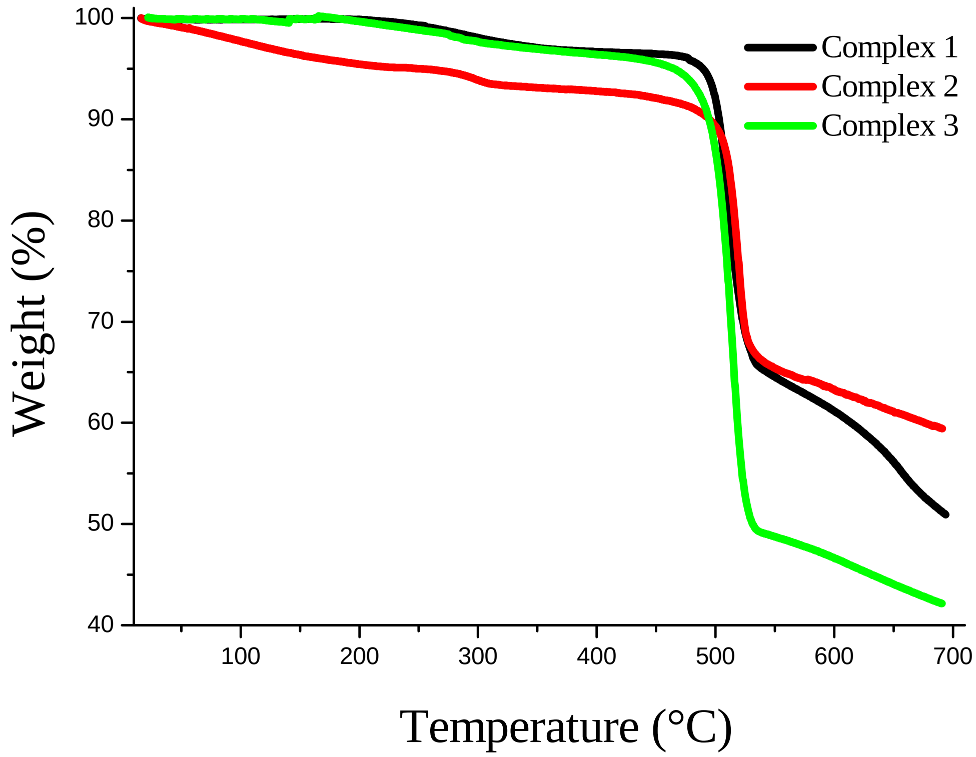

Figure S2. The TGA curves of **1 - 3**.

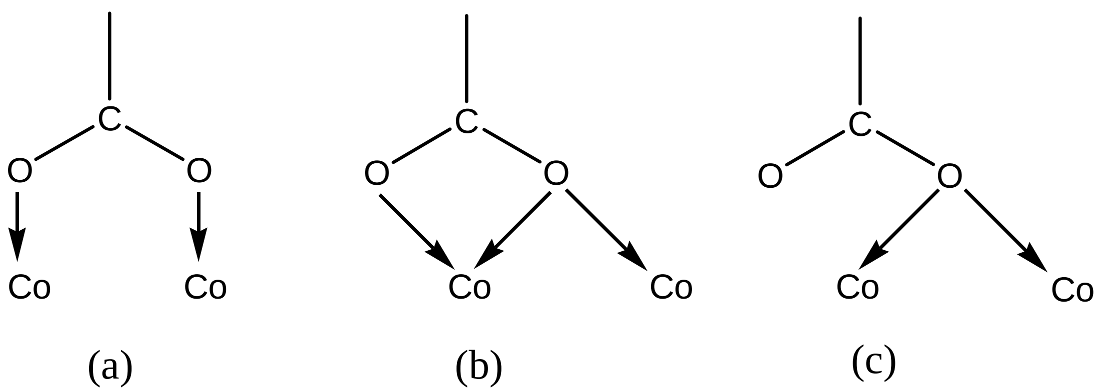

Figure S3. Modes of carboxylic groups of CTC^{3-} in **1**: Bidentate (a), Chelating/Bridging Bidentate (b) and Bridging Unidentate (c).

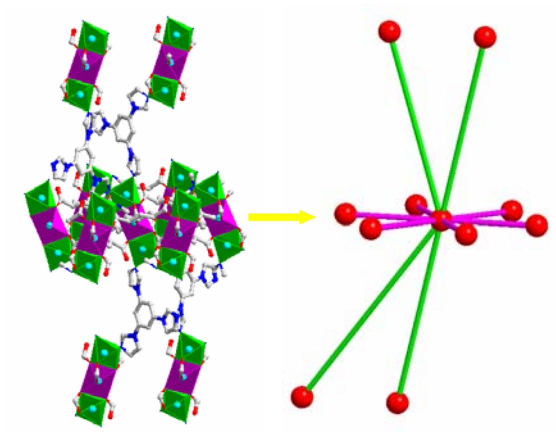

Figure S4. Ball-stick and polyhedral (left) and simplified (right) view of the 10-connected node.

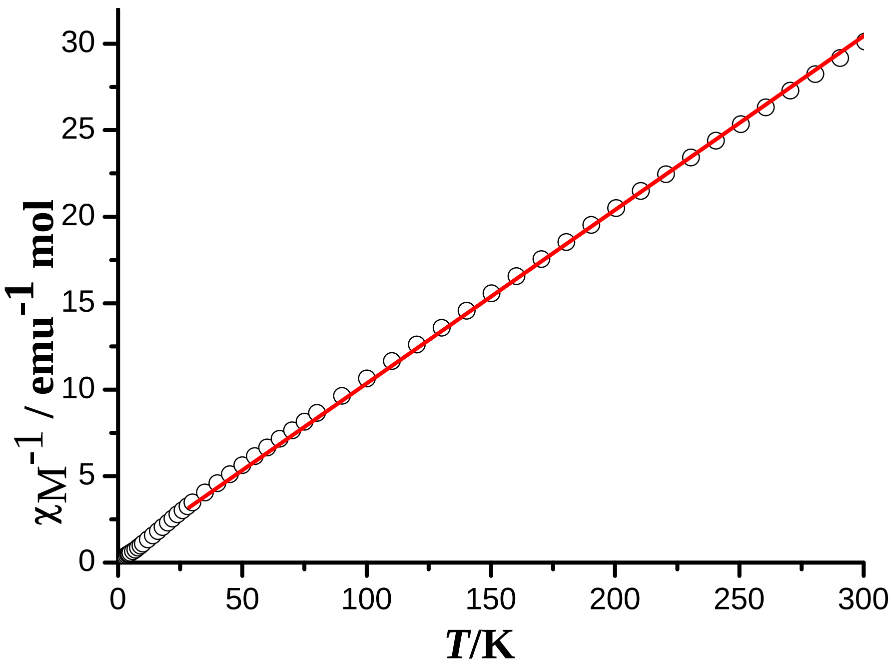

Figure S5. Plot of χ_M^{-1} *vs* T in the range of 1.8-300 K for **1**, the solid line is the linear fitting based on the Curie-Weiss law.

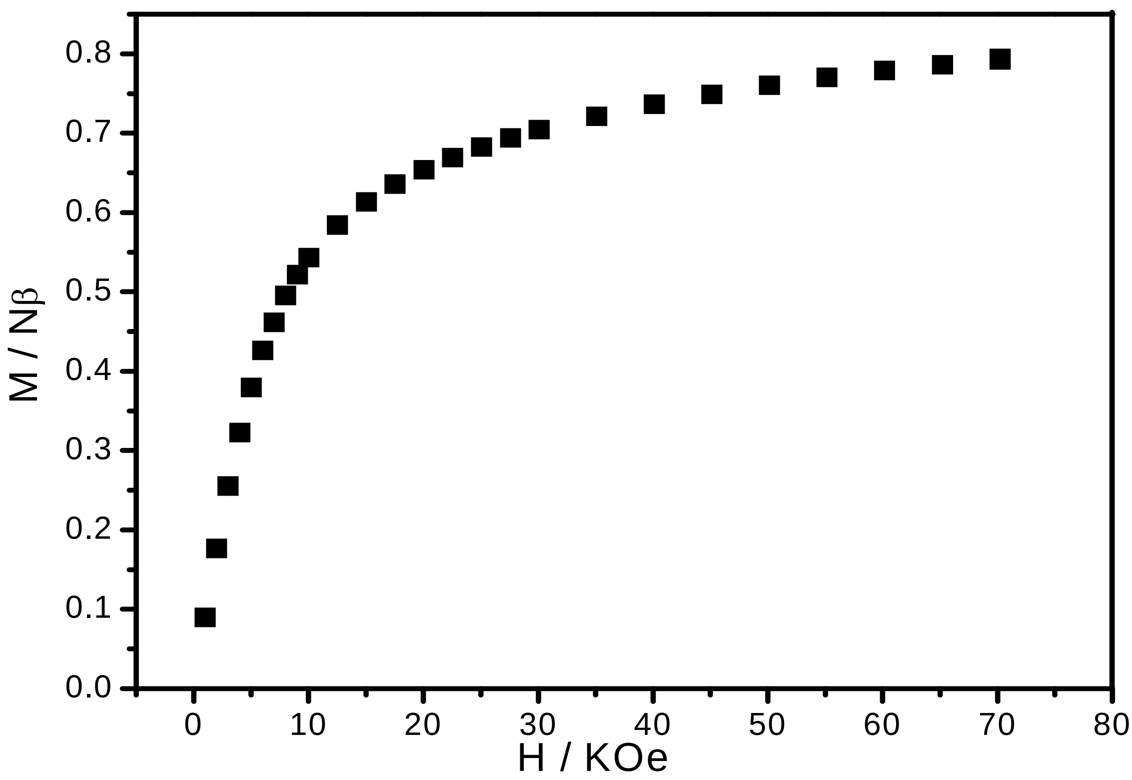

Figure S6. The plot of magnetization versus applied magnetic field of **1** at 1.8 K.

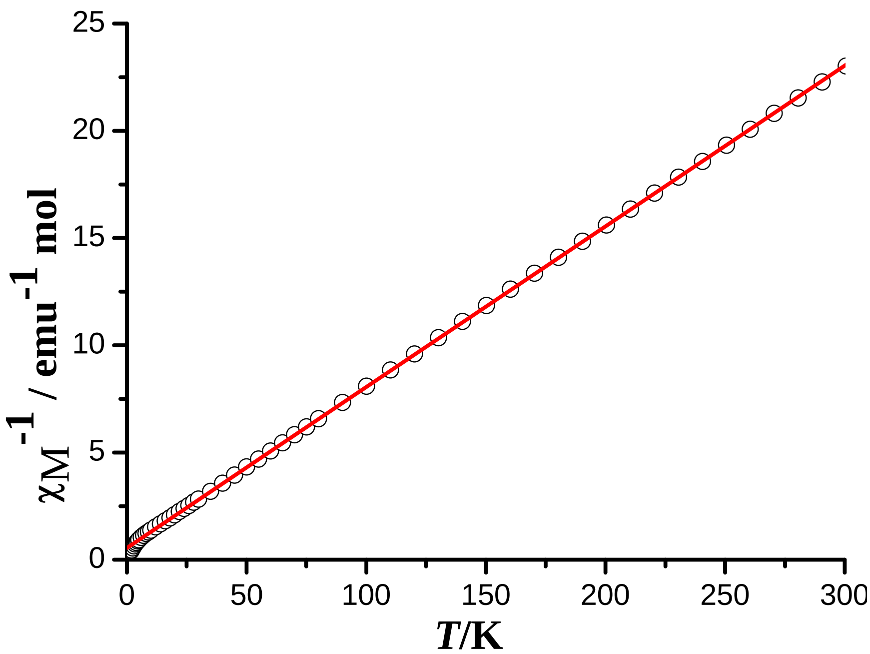

Figure S7. Plot of χ_M^{-1} *vs* T in the range of 1.8-300 K for **2**, the solid line is the linear fitting based on the Curie-Weiss law.

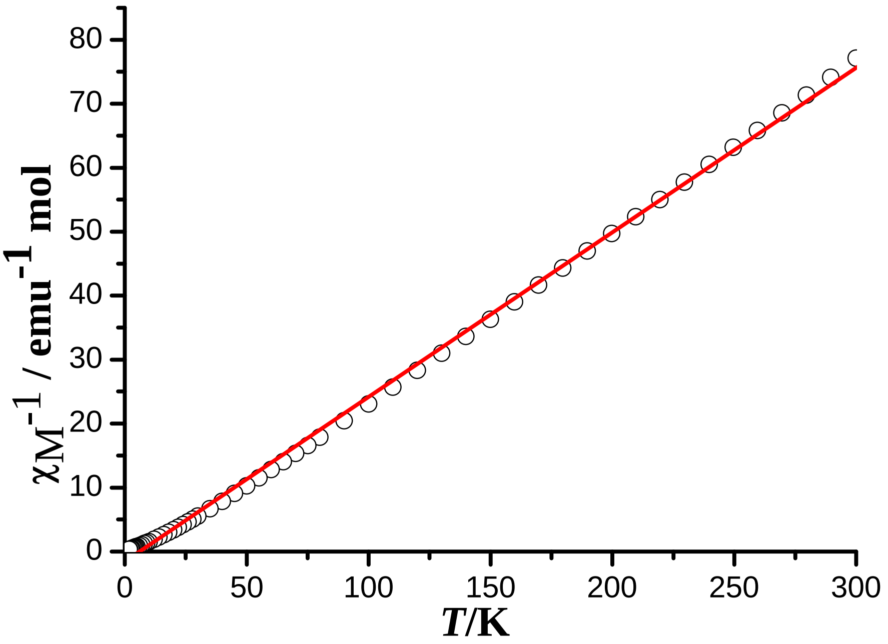

Figure S8. Plot of χ_M^{-1} *vs* T in the range of 1.8-300 K for **3**, the solid line is the linear fitting based on the Curie-Weiss law.

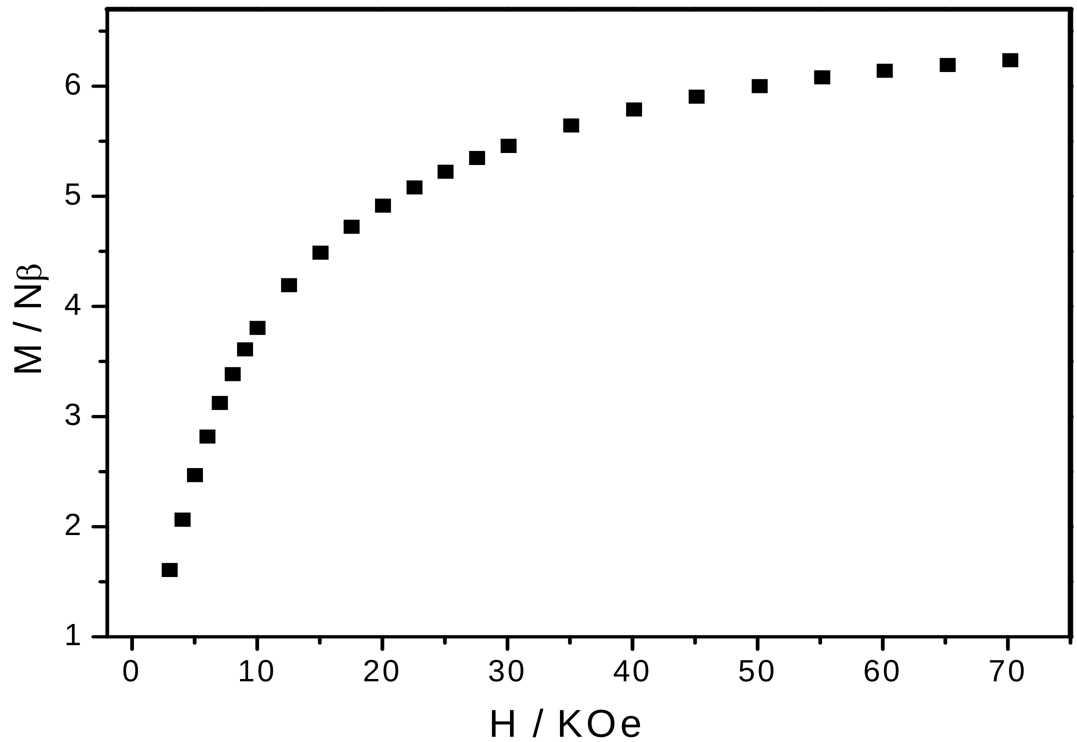

Figure S9. The plot of magnetization versus applied magnetic field of **3** at 1.8 K.

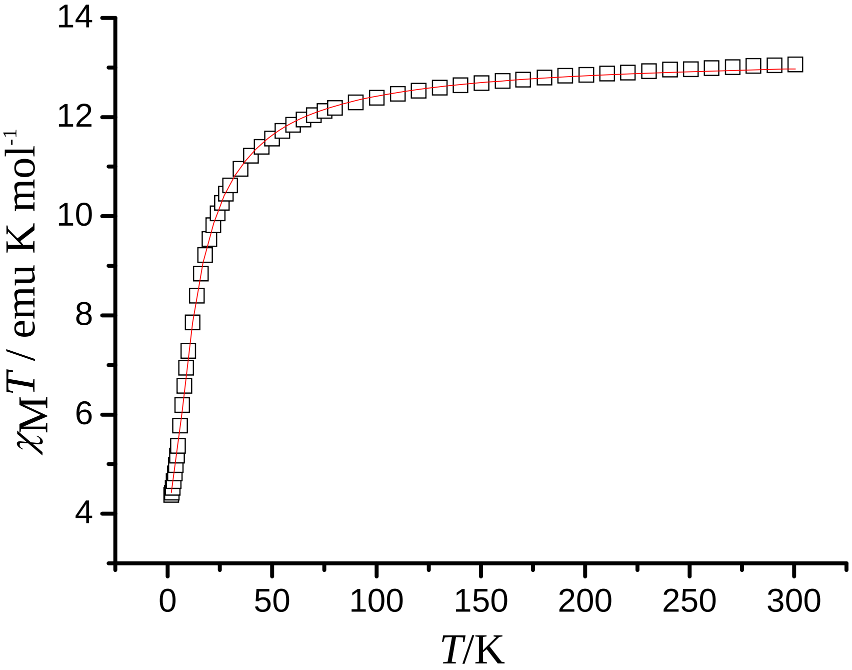

Figure S10. The plot of $\chi_M T$ *vs.* T for **2**, where the solid line represents the fitted curve without considering the *zj*' component.

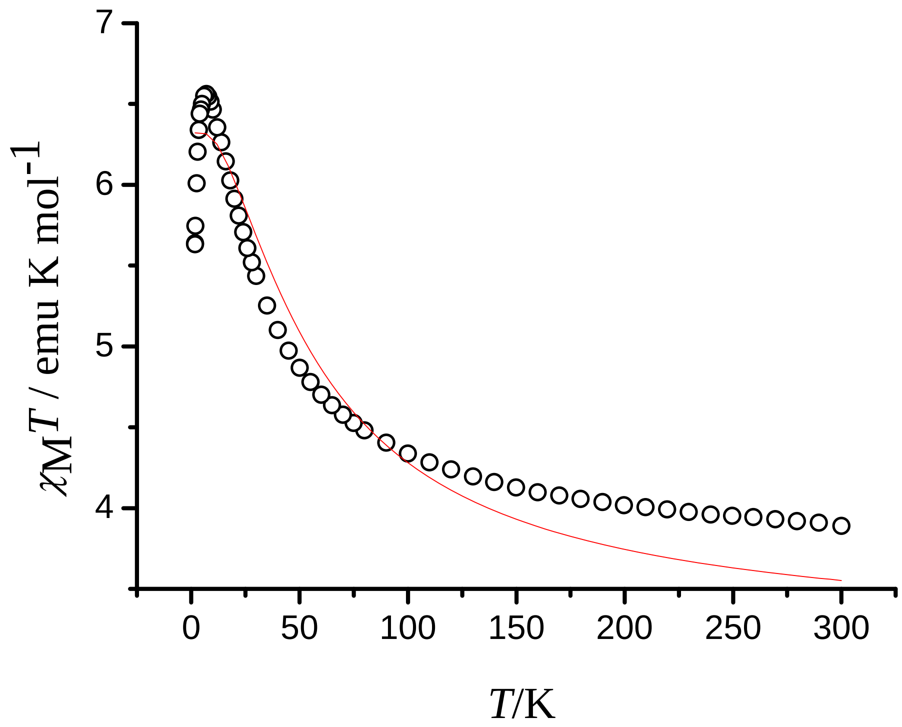

Figure S11. The plot of $\chi_M T$ *vs.* T for **3**, where the solid line represents the fitted curve without considering the *zj*' component.

$$
\begin{aligned}
A &= 105/2 + 1020\exp(25J/kT) + 1365/2\exp(20J/kT) + 429\exp(15J/kT) \\
&+930\exp(10J/kT) + 429\exp(7J/kT) + 126\exp(5J/kT) + 495/2\exp(4J/kT) \\
&+126\exp(J/kT) + 105/2\exp(-2J/kT) + 429\exp(-3J/kT) + 495/2\exp(-4J/kT) \\
&+126\exp(-5J/kT) + 105/2\exp(-6J/kT) + 15\exp(-7J/kT) + 15\exp(-11J/kT) \\
&+105/2\exp(-12J/kT) + 126\exp(-13J/kT) + 249\exp(-14J/kT) + 15\exp(-17J/kT) \\
&+54\exp(-20J/kT) + 126\exp(-23J/kT) + 15\exp(-25J/kT) + 105/2\exp(-30J/kT)
\end{aligned}
$$

$$
\begin{aligned}
B &= 6 + 16\exp(25J/kT) + 14\exp(20J/kT) + 12\exp(15J/kT) + 24\exp(10J/kT) \\
&+12\exp(7J/kT) + 8\exp(5J/kT) + 10\exp(4J/kT) + 8\exp(J/kT) + 6\exp(-2J/kT) \\
&+12\exp(-3J/kT) + 10\exp(-4J/kT) + 8\exp(-5J/kT) + 6\exp(-6J/kT) + 4\exp(-7J/kT) \\
&+4\exp(-11J/kT) + 6\exp(-12J/kT) + 8\exp(-13J/kT) + 12\exp(-14J/kT) + 4\exp(-17J/kT) \\
&+8\exp(-20J/kT) + 8\exp(-23J/kT) + 4\exp(-25J/kT) + 6\exp(-30J/kT)
\end{aligned}
$$

Scheme S1. The meaning of A and B in equation 5.

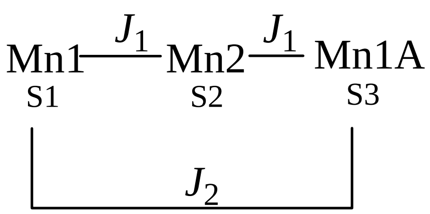

Scheme S2. Exchange integrals in trinuclear Mn(II) motif of **2**.

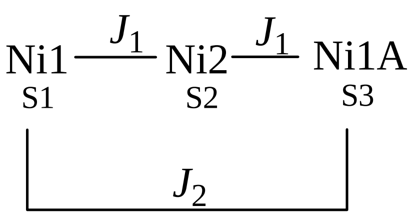

Scheme S3. Exchange integrals in trinuclear Ni(II) unit of **3**.